

# Nanostructures Formed by Self-Assembly of Negatively Charged Polymer and Cationic Surfactants

G. Nizri,<sup>†</sup> A. Makarsky,<sup>‡</sup> S. Magdassi,<sup>\*,†</sup> and Y. Talmon<sup>‡</sup>

Casali Institute of Applied Chemistry, The Hebrew University of Jerusalem, Jerusalem 91904, Israel, and  
Department of Chemical Engineering, Technion-Israel Institute of Technology, Haifa 32000, Israel

Received September 22, 2008. Revised Manuscript Received November 24, 2008

The formation of nanoparticles by interaction of an anionic polyelectrolyte, sodium polyacrylate (NaPA), was studied with a series of oppositely charged surfactants with different chain lengths, alkyltrimethylammonium bromide ( $C_n$ TAB). The binding and formation of nanoparticles was characterized by dynamic light scattering,  $\zeta$ -potential, and self-diffusion NMR. The inner nanostructure of the particles was observed by direct-imaging cryogenic-temperature transmission electron microscopy (cryo-TEM), indicating aggregates of hexagonal liquid crystal with nanometric size.

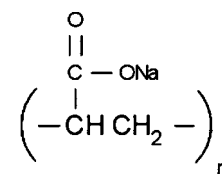
## Introduction

Aqueous solutions containing polymers and surfactants are common in biological systems and various industrial applications; hence, it is important and useful to understand the nature of interaction between the components of such systems. It was previously recognized that surfactants in solution tend to bind to polymers.<sup>1–5</sup> The process starts at a well defined surfactant concentration denoted as the critical aggregation concentration, CAC. It was experimentally observed that this CAC is much lower than the critical micellization concentration, CMC, of the surfactant solution.<sup>6</sup>

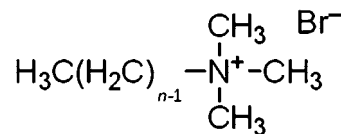
In systems containing a charged polymer and an oppositely charged surfactant, phase separation usually occurs due to strong electrostatic forces. At a certain surfactant concentration range this leads eventually to precipitation of a polymer–surfactant complex. This precipitation has been characterized for various oppositely charged polyelectrolyte–surfactant systems, mainly from a point of view of the bulk dispersion behavior, by measuring the conductivity, surface tension, calorimetry, and rheology.<sup>7–12</sup> However, it has been found that binding of the surfactant to the polymer could occur without precipitation, while small dispersed complexes are formed.<sup>13</sup>

In a previous paper<sup>14</sup> we characterized the interaction between an anionic surfactant, SDS, and a polycation, PDAC (polydi-

Chart 1



NaPA



$C_n$ TAB

allyldimethylammonium chloride). We found that nanoparticles were formed in that system at various surfactant/polymer charge ratios, and their inner structure was similar to a hexagonal liquid crystal. In the present work we show that these findings are also valid in systems composed of negatively charged polymer and positively charged surfactants. We evaluated the interactions between a negatively charged polymer (sodium polyacrylate, NaPA) and a series of cationic surfactants ( $C_n$ TAB), shown in Chart 1. The formation of nanoparticles was evaluated for surfactants with different chain lengths and at a wide range of surfactant/polymer charge ratios for the  $C_{16}$ TAB–NaPA system.

The interaction between poly(acrylic acid) (in its protonated form) and  $C_{16}$ TAB in aqueous solution was previously investigated and found to be strongly dependent on pH and charge ratio between the polymer and surfactant.<sup>15</sup> In addition, Ilekli et al.<sup>16</sup> studied the interaction between  $C_{16}$ TAB and NaPA in a molar charge ratio of 1, which caused phase separation. It was concluded, based on elemental analysis and SAXS measurements, that the association resulted from an ion-exchange process, and that  $C_{16}$ TAB formed elongated micelles in the presence of NaPA. Phase diagrams for a preformed complex of  $C_{16}\text{TA}^+$  and polyacrylate solutions (CTAPA, formed by titrating hexadecyl-

\* Corresponding author.

<sup>†</sup> The Hebrew University of Jerusalem.

<sup>‡</sup> Technion-Israel Institute of Technology.

(1) Winnik, F.; Regismond, S. T. A.; Picullel, L.; Lindman, B.; Karlstrom, G.; Zana, R. In *Polymer-Surfactant Systems*; Kwak, J. C. T., Eds.; Dekker: New York, 1998; Vol. 77, pp 65–142, 267–316, 409–454.

(2) Goddard, E. D.; Ananthapandmanabhan, K. P. *Interactions of Surfactants with Polymers and Proteins*; CRC Press: Boca Raton, FL, 1993.

(3) Cabane, B.; Duplessix, R. *Colloids Surf.* **1985**, *13*, 19.

(4) Lindman, B.; Thalberg, K. In *Polymer-Surfactant Interactions*; Goddard, E. D., Ananthapandmanabhan, K. P., Eds.; CRC Press: Boca Raton, FL, 1993; p 203.

(5) Thüнемann, A. F. *Prog. Polym. Sci.* **2002**, *27*, 1473.

(6) Kogej, K.; Škerjanc, J. *Langmuir* **1999**, *15*, 4251.

(7) Campbell, R. A.; Ash, P. A.; Bain, C. D. *Langmuir* **2007**, *23*, 3242.

(8) Muzzalupo, R.; Infante, M. R.; Pe'rez, L.; Pinazo, A.; Marques, E. F.; Antonelli, M. L.; Strinati, C.; La Mesa, C. *Langmuir* **2007**, *23*, 5963.

(9) Chakraborty, T.; Chakraborty, I.; Ghosh, S. *Langmuir* **2006**, *22*, 9905.

(10) Mata, J.; Patel, J.; Jain, N.; Ghosh, G.; Bahadur, P. J. *Colloid Interface Sci.* **2006**, *297*, 797.

(11) Penfold, J.; Tucker, I.; Thomas, R. K.; Taylor, D. J. F.; Zhang, J.; Zhang, X. L. *Langmuir* **2007**, *23*, 3690.

(12) Kong, L.; Cao, M.; Hai, M. J. *Chem. Eng. Data* **2007**, *52*, 721.

(13) Dubin, P. L.; Oteri, R. J. *Colloid Interface Sci.* **1983**, *95*, 453.

(14) Nizri, G.; Magdassi, S.; Schmidt, J.; Cohen, Y.; Talmon, Y. *Langmuir* **2004**, *20*(11), 4380.

(15) Fundin, J.; Hansson, P.; Brown, W.; Lidegran, I. *Macromolecules* **1997**, *30*, 1118.

(16) Ilekli, P.; Picullel, L.; Tournilhac, F.; Cabane, B. *J. Phys. Chem. B* **1998**, *102*, 344.

trimethylammonium hydroxide with poly(acrylic acid)) with  $C_{16}TAB$  and no  $Na^+$  ions were studied by Svensson et al.<sup>17</sup> It was found by SAXS that several different phases were formed in this system, while a hexagonal phase was formed over a wide range of concentrations. CTAPA was also investigated by Norrman et al.<sup>18</sup> from the point of view of the effect of inserting uncharged monomers into the polyion of the complex using poly(acrylic acid); it was concluded that the charge density of the polymer strongly affected the size and shape of CTAPA complex.

The present research provides a comprehensive study on formation of nanoparticles by the interaction of a polyanion and a series of cationic surfactants, at various molar charge ratios. This study also presents, for the first time, direct observations of the inner structure of nanoparticles formed by the interaction of NaPA and  $C_nTAB$  surfactants.

### Experimental Section

**Materials.** NaPA (15 000 g/mol MW) was purchased from Sigma-Aldrich as a 35% w/w aqueous solution. The surfactants  $C_nTAB$  ( $n = 8, 10, 12, 14, 16$ ) were purchased from Sigma-Aldrich as 99% pure powders and were used without further purification.

**Sample Preparation.** Aqueous stock solutions of the surfactants were prepared by weighing the required amount of dry substance. Polymer stock solutions were prepared by diluting the original 35% w/w polymer solution. For each sample, stock solutions of the polymer and surfactant were prepared so that the concentrations were double the required concentration needed in the sample. Equal volumes of the two solutions were then poured simultaneously into a vial while stirring, so that the final concentration of each component was a half of that of the stock solution used. After the solutions were mixed, the resulting dispersion was turbid at certain concentrations. The dispersions were stirred by a magnetic stirrer for 30 min, followed by storage for 24 h, before any measurement was taken.

**Size and  $\zeta$ -Potential.** Zeta-potential measurements were performed with a ZetaMaster 3000 (Malvern Instruments). Size measurements were performed by dynamic light scattering (NanoSZ, Malvern Instruments), and the average size by number are presented. Dispersions of  $C_nTAB$ -NaPA were placed in a cuvette and measured without dilution. All samples were prepared in duplicates; each measurement was performed three times. The calculation of size distribution from light scattering measurements is based on the assumption that the particles are spherical. Because the nanoparticles are not ideal spheres, as shown by cryo-TEM, the size measurements give only relative values rather than absolute size. The  $\zeta$  potential was calculated automatically from the measured electrophoretic mobility, by the Henry equation:  $Ue = \epsilon \zeta f / 6\pi\eta$  where  $Ue$  is the electrophoretic mobility,  $\epsilon$  is the dielectric constant,  $\eta$  is the viscosity, and  $\zeta$  is the zeta potential. The Smoluchowski factor,  $f = 1.5$ , was used for the conversion of mobility to  $\zeta$  potential.<sup>19</sup> Samples at low surfactant concentrations were concentrated by ultrafiltration (100 kDa, Millipore) prior to the measurement, to improve signal during zeta potential measurements.

**Cryo-TEM.** Vitrified specimens for cryo-TEM were prepared in a controlled environment vitrification system (CEVS), where temperature and saturation were controlled. A drop of the sample was placed on a perforated carbon film-coated copper grid, blotted with filter paper, and plunged into liquid ethane at its freezing point. The vitrified specimen was transferred to an Oxford CT-3500 cooling holder and observed in a Philips CM120 transmission electron microscope at about  $-180$  °C in the low-dose imaging mode to

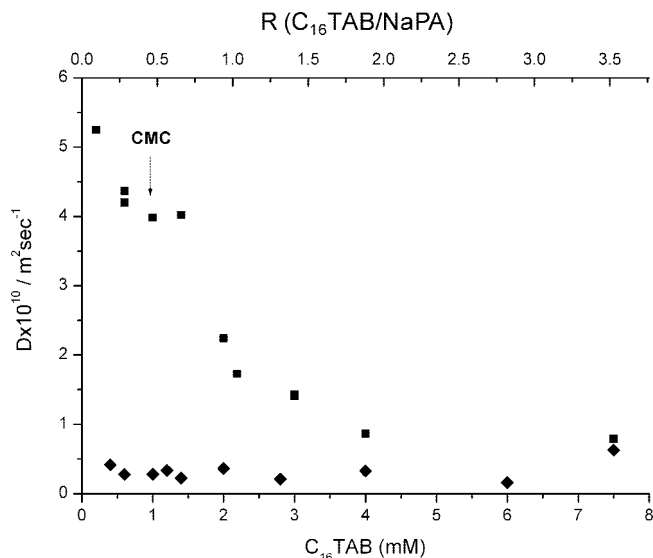


**Figure 1.** Diffusion coefficients of  $C_{16}TAB$  in the absence (■) and the presence (◆) of NaPA (0.02%, 2.13 mM) as a function of  $C_{16}TAB$  concentration.

minimize electron-beam radiation damage. Images were digitally recorded with a Gatan 791 MultyScan CCD camera. More details of the methodology may be found elsewhere.<sup>20,21</sup>

**NMR Self-Diffusion.** NMR measurements were performed at 25 °C with a Bruker DRX-400 spectrometer with BGU II gradient amplifier unit, and a 5 mm BBI probe equipped with a z-gradient coil, providing a z-gradient strength ( $g$ ) of up to  $55 G \cdot cm^{-1}$ . The self-diffusion coefficients were determined using bipolar-pulsed field gradient stimulated spin-echo (BPGF-SSE). Experiments were carried out by varying  $g$  and keeping all other timing parameters constant. The self-diffusion coefficient ( $D$ ) is given by:

$$I = I_0 / 2 e^{-R(t) - (\gamma G \delta) 2D(\Delta - \delta)} \quad (1)$$

where  $I$  is the measured signal intensity,  $I_0$  is the signal intensity for  $g = 0$ ,  $\gamma$  is the gyromagnetic ratio for the  $^1H$  nucleus,  $\delta$  is the gradient pulse length,  $\Delta$  is the time between the two gradients in the pulse sequence (and hence defines the diffusion time), and  $R(t)$  is a constant that takes into account nuclear relaxation. Because in our experiments  $R(t)$  was constant, we did not consider it further. Typical experiments used a  $\Delta$  of 100 ms, a  $\delta$  of 8 ms, and  $g$  values from 1.7 to  $32.3 G \cdot cm^{-1}$  in 32 steps.

### Results and Discussion

**Binding of Surfactant to the Polymer.** An indication of the interaction between the surfactant and the polymer was obtained from self-diffusion NMR of the system  $C_{16}TAB$ -NaPA. In this paper we focused on the interaction between NaPA and  $C_{16}TAB$  since this system leads to the formation of the most ordered structures, as seen below from cryo-TEM images. However, in the future it would be interesting to investigate the effect of surfactant chain length on the diffusion coefficients. In Figure 1 the diffusion coefficients of  $C_{16}TAB$  in the presence and in the absence of NaPA are plotted as function of  $C_{16}TAB$  concentration and molar charge ratio (in the presence of polymer). The diffusion coefficients of  $C_{16}TAB$  in the absence of polymer are similar to the values previously reported by Cabaleiro-Lago et al.<sup>22</sup> ( $\sim 4 \times 10^{-10} m^2 s^{-1}$  below the cmc of  $C_{16}TAB$ ), and Walderhaug et

(17) Svensson, A.; Piculell, L.; Cabane, B.; Ilkkti, P. *J. Phys. Chem. B* **2002**, *106*, 1013.

(18) Norrman, J.; Lynch, I.; Piculell, L. *J. Phys. Chem. B* **2007**, *111*, 8402.

(19) Shaw, D. J. *Introduction to Colloid and Surface Chemistry*, 4th ed.; Butterworth-Heinemann Ltd.: Oxford, U.K., 1991; p 202.

(20) Bellare, J. R.; Davis, H. T.; Scriven, L. E.; Talmon, Y. *J. Electron Microsc. Technol.* **1988**, *10*, 87.

(21) Talmon, Y. In *Giant Micelles*; Zana, R., Kaler, E.A., Eds.; CRC Press: New York, 2007; chapter 5, pp 163–178.

(22) Cabalero-Lago, C.; Nilsson, M.; Soderman, O. *Langmuir* **2005**, *21*, 11637.

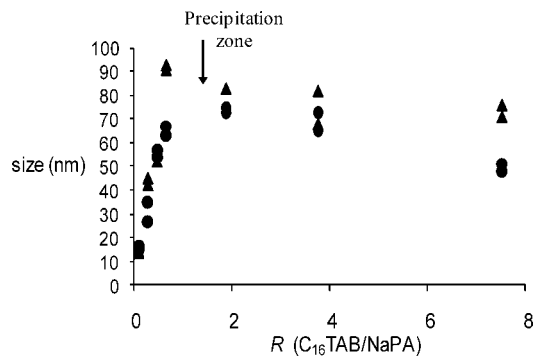


**Figure 2.** Number-average size, measured by dynamic light scattering, of  $C_{16}TAB$ –NaPA at 0.01% NaPA (15 000 Da), 0.1–8 mM  $C_{16}TAB$  (●), and 0.02% NaPA (15 000 Da), 0.2–16 mM  $C_{16}TAB$  (▲), as a function of  $R$ .

al.<sup>23</sup> ( $\sim 0.9 \times 10^{-10} \text{ m}^2 \text{ s}^{-1}$  for  $C_{16}TAB$  at 4 mM, above the CMC). As expected, with the increase in surfactant concentration, the diffusion coefficient abruptly decreases at a certain surfactant concentration as a consequence of micellization, and keeps decreasing, probably due to micelles growing, in agreement with the results of Mata et al.<sup>24</sup> As shown, in presence of NaPA at low  $C_{16}TAB$  concentrations, the diffusion coefficients of  $C_{16}TAB$  are much smaller than the values obtained for the surfactant alone. This indicates binding of the surfactant to the polymer, which reduces the mobility of surfactant molecules. At higher surfactant concentrations (leading to high molar charge ratio,  $R$ , between the surfactant and polymer), e.g.,  $R = 3.5$ , there is excess of free surfactant micelles in the dispersion, and the diffusion coefficients are close to those obtained for  $C_{16}TAB$  micelles alone.

The hydrodynamic diameter of the complexes formed between the surfactant and the polymer was calculated for the system at 1 mM  $C_{16}TAB$  ( $R = 0.47$ ) using the Stokes–Einstein equation.<sup>25,26</sup>

$$D_H = 2kT/6\pi\eta D \quad (2)$$

where  $D_H$  is the hydrodynamic diameter,  $k$  is Boltzmann's constant,  $T$  is the absolute temperature,  $\eta$  is the viscosity, and  $D$  is the measured diffusion coefficient. A value of  $\sim 10$  nm was obtained for this composition ( $R = 0.47$ ). For comparison, the particle size measured for this ratio by DLS is higher, around 50 nm (see Figure 2). For 50 nm particles the diffusion coefficient should be  $8.7 \times 10^{-11} \text{ m}^2 \text{ s}^{-1}$  (the diffusion coefficient is calculated from the NMR peak of the  $C_{16}TAB$ ), a value much smaller than the ones found for the nanoparticles by the NMR measurements. This difference can be explained by the coexistence of free surfactant molecules, micelles, and particles in the dispersion. Since the micelles can be hardly detected by the light scattering instrument, larger average particle size is obtained. Also the micelle population is detected by the SD-NMR, yielding a larger diffusion coefficient than for the particles alone, thus yielding a smaller average particle size.

The particle formation process was followed by dynamic light scattering (DLS) measurements of samples containing  $C_{16}TAB$  at  $R$  values of 0.47 and 7.52, NaPA 0.01% w/w. Measurements were taken immediately after mixing up to 1 h from initial mixing, every few seconds. The nanoparticles in both samples were of

the size  $\sim 40$  nm, and it was found that they reached their final size immediately after mixing, and that no significant change occurred within 1 h, neither in the average size by number distribution, nor in the polydispersity index value, which represents the width of the particle size distribution. In addition, in order to follow the particle stability with time, size measurements were performed up to 100 days after preparation. It was found that there was no significant change in their average size or polydispersity index.

**Effect of Molar Charge Ratio.** We evaluated the effect of the surfactant/polymer molar charge ratio on particle size. The dynamic light scattering results shown in Figure 2 indicate that particles in the size range of 10–100 nm are formed in a wide range of charge ratios ( $R = 0.094$ –7.65). In general, the particle size increased with the increase in charge ratio, up to  $R = 1$ , when precipitation was observed. As expected, at  $R = 1$ , charge neutralization occurred, which led to precipitation. Above that charge ratio, the particle size decreased slightly, due to the higher ionic strength as the surfactant concentration increases, which led to less favorable electrical interaction of the surfactant with the polymer. Note that higher concentrations of the polymer (0.02% compared to 0.01% w/w) led to formation of slightly larger particles at large  $R$  values, probably due to the enhanced possibility of aggregation of the particles.

One cannot exclude the possibility that the particles are simply formed due to aggregation caused by the presence of electrolytes (through the counterions). Therefore, we conducted a control experiment, in which NaBr was added to a  $C_{16}TAB$  solutions, instead of the polyelectrolyte (at concentration similar to 0.02% w/w polymer, 2 mM monomeric units of the polymer, which corresponds to  $R = 7.65$ ). In another control experiment we added NaBr (at a concentration similar to the surfactant concentration, 15 mM, which corresponds to  $R = 7.65$ ) to 0.02% w/w NaPA solution. In both cases, particles were not formed, as verified by turbidity and DLS measurements. This contradicts the results obtained by Svensson et al.<sup>27</sup> according to computer simulations that showed that the effect of added NaPA to CTAPA is similar to the effect caused by the addition of a simple electrolyte, from the point of view of the aggregate surface charge.

The process of charge interactions and neutralization can be followed by measuring the  $\zeta$  potential of the particles. The particles could have either a positive or negative surface potential, depending on the surfactant-to-polymer charge ratio. Indeed, as shown in Figure 3, the  $\zeta$  potential is negative for charge ratios below 1, and the absolute value decreases with the increase of  $R$ . At  $R$  values higher than 1, the  $\zeta$  potential is positive. At  $R \sim 1$ , charge neutralization occurs, and the potential is indeed close to zero. At  $R$  ratios above 1, excess surfactant is bound to the polymer–surfactant complex and contributes to particles positive charge.

The effect of charge molar ratio on the inner structure of the particles was evaluated by cryo-TEM from a series of samples with increasing molar charge ratios of  $C_{16}TAB$  to NaPA. At  $R = 0.094$  and 0.282, the  $C_{16}TAB$  concentration is below the CMC of pure  $C_{16}TAB$  (0.98 mM).<sup>28</sup> The number of particles at these surfactant concentrations was very small, and a wide range of particles sizes was observed. The systems showed typical particles of well-ordered domains, as shown in Figure 4a,b. The particles have well defined edges with an approximately  $120^\circ$  angle between them. The apparent angle deviated occasionally from  $120^\circ$ , because of the position of particle relative to the electron

(23) Walderhaug, H.; Nystroem, B.; Hansen, F. K.; Lindman, B. *J. Phys. Chem.* **1995**, *99*(13), 4672.

(24) Mata, J.; Varade, D.; Bahadur, P. *Thermochim. Acta* **2005**, *428*, 147.

(25) Johnson, C. S. *Prog. Nucl. Magn. Reson. Spectrosc.* **1999**, *34*, 203.

(26) Maklakov, A. I.; Skirda, V. N.; Fatkullin, N. F. In *Self-Diffusion in Polymer Solutions and Melts*; Kazan. Gos. Univ.: Kazansk, 1987.

(27) Svensson, A.; Piculell, L.; Karlsson, L.; Cabane, B.; Jönsson, B. *J. Phys. Chem. B* **2003**, *107*, 8119.

(28) Rosen, M. J. *Surfactants and Interfacial Phenomena*, 3rd ed.; John Wiley & Sons: Hoboken, NJ, 2004, p 128.

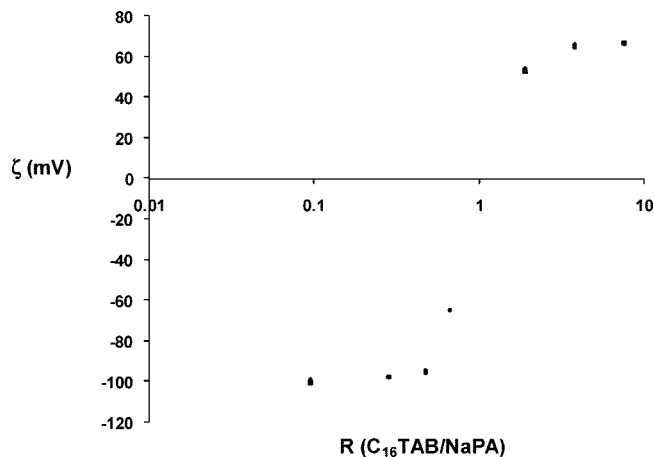


**Figure 3.**  $\zeta$  potential of C<sub>16</sub>TAB–NaPA series at 0.02% NaPA (15 000 Da) as a function of  $R$ . C<sub>16</sub>TAB concentration 0.2–16 mM.

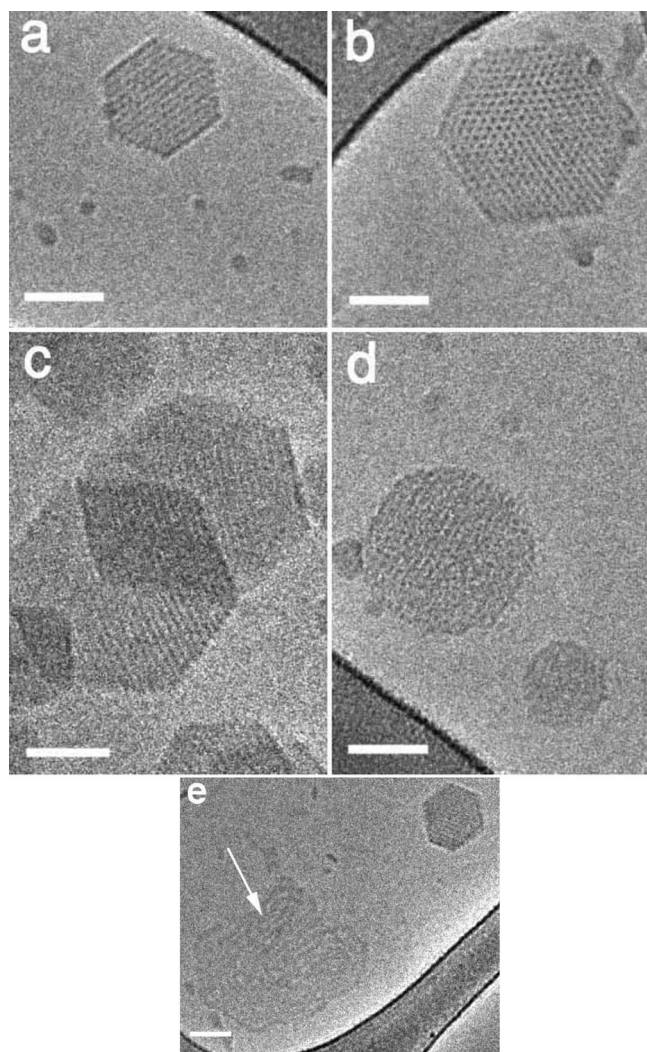


**Figure 4.** Cryo-TEM images of nanoparticles formed by C<sub>16</sub>TAB and NaPA (0.02%) at various surfactant-to-polymer ratio: (a)  $R = 0.094$  (0.2 mM C<sub>16</sub>TAB); (b)  $R = 0.282$  (0.6 mM C<sub>16</sub>TAB); (c, e)  $R = 0.47$  (1 mM C<sub>16</sub>TAB); (d)  $R = 0.658$  (1.4 mM C<sub>16</sub>TAB). Scale bars = 50 nm.

beam. This structure strongly suggests hexagonal liquid crystal particles. In addition, the well ordered round objects within the nanoparticle in Figure 4b are quite probably a cross-section view of threadlike micelles (TLMs), suggesting that these polymer–surfactant complexes are indeed hexagonal liquid crystal particles.

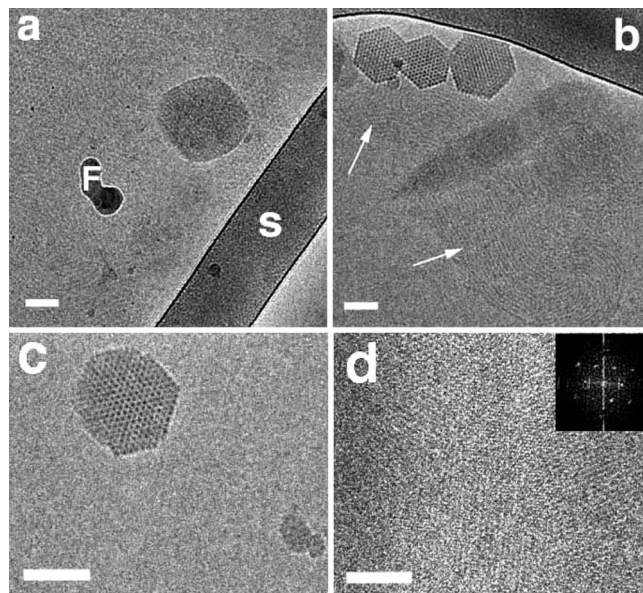


**Figure 5.** Cryo-TEM images of nanoparticles formed by C<sub>16</sub>TAB and NaPA (0.02%) at different surfactant-to-polymer ratio: (a)  $R = 1.88$  (4 mM C<sub>16</sub>TAB); (b)  $R = 3.25$  (6.9 mM C<sub>16</sub>TAB); (c, d)  $R = 7.65$  (16 mM C<sub>16</sub>TAB). Scale bars = 50 nm. Arrows in ‘b’ point to fingerprint pattern. ‘F’ in ‘a’ indicates a frost particle, ‘S’ indicates the support film.

We observed similar structures at  $R = 0.470$  and  $0.658$  (Figures 4c and 4d; many more particles were observed at the higher  $R$  value). At the higher  $R$  value, many of the aggregates tended to have less sharp edges, e.g., the lower particle in Figure 4d. Interestingly, in addition to the particles of the hexagonal symmetry, at  $R = 0.470$  we observed coexisting threadlike micelles arranged in spirals (Figure 4e). TLMs are building blocks of the hexagonal liquid crystal particles.

At  $R = 1.88$  and  $3.25$ , hexagonal nanostructured particles are seen again (Figure 5a,b), along with fainter, larger, “fingerprint” patterns (arrows in Figure 5b) of TLMs. In the upper left corner of Figure 5a an ordered domain of hexagonal symmetry is clearly seen. In this figure, merging of separate particles into a larger particle is observed. Finally at  $R = 7.65$ , the system showed both hexagonal nanoparticles (Figure 5c) and very large domains of ordered structure (Figure 5d). The inset in the latter figure is the Fourier transform of an area within the main micrograph. It shows clearly the long-range order in that domain. Such hexagonal liquid crystalline structure was also obtained by the interaction of alkyltrimethylammonium bromides and the anionic bile salt, sodium desoxycholate, studied by X-ray diffraction and fluorescence quenching by Vethamuthu et al.<sup>29</sup>

It is worth noting that C<sub>16</sub>TAB in water is reported to form threadlike micelles only at higher concentrations, around 0.25 M (at 30 °C).<sup>30</sup> However, in our system TLMs are seen at much lower C<sub>16</sub>TAB concentrations. Thus, it can be assumed that the polymer induces the formation of C<sub>16</sub>TAB cylindrical micelles. The hexagonal liquid crystal particles we observe could be made up of C<sub>16</sub>TAB cylindrical micelles decorated by NaPA molecules, arranged along the long axis of the cylinders. The model we suggested in the past for the case of positively charged polymer and an anionic surfactant<sup>14</sup> may be applicable to this system too. The COO<sup>−</sup> groups on the polymer chain may act as a salt screening the electric charges of the positively charged ammonium groups.

(29) Vethamuthu, M. S.; Almgren, M.; Bergenstål, B.; Mukhtar, E. *J. Colloid Interface Sci.* **1996**, *178*, 538.

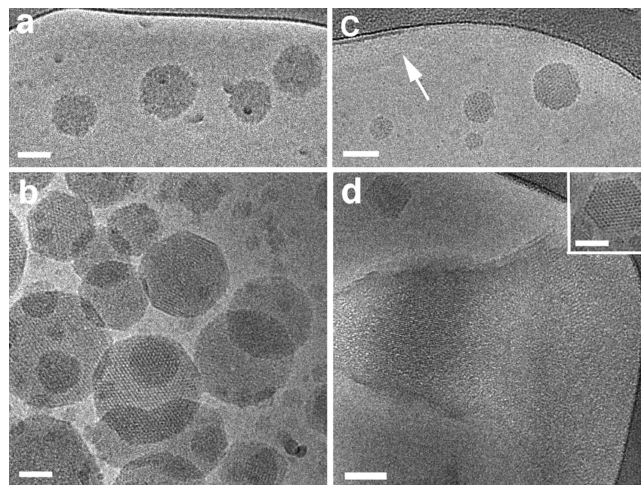
(30) Panchal, K. N.; Desai, A.; Nagar, T. *J. Dispers. Sci. Technol.* **2006**, *27*, 963.

**Table 1.** C<sub>n</sub>TAB–NaPA Nanoparticle Size at  $R = 0.47$ , NaPA 0.1% (10 mM based on the monomeric unit), Surfactant Concentration 5 mM

surfactant	average size by number distribution (nm)	polydispersity index (PDI)
C <sub>8</sub> TAB	no particles	
C <sub>10</sub> TAB	4.5 ± 0.25	0.54 ± 0.05
C <sub>12</sub> TAB	54 ± 1	0.14 ± 0.00
C <sub>14</sub> TAB	76 ± 2	0.145 ± 0.50
C <sub>16</sub> TAB	88.5 ± 10	0.16 ± 0.01

The proximity of those groups along the polymer chains makes such alignment quite probable. It is known that salts induce formation of the lower-curvature aggregates. For example, spherical micelles of C<sub>16</sub>TAB become rodlike or wormlike when KBr at 0.1 or 0.2 M is added.<sup>31</sup> It is also known that the interaction between a polyelectrolyte-neutral block copolymer with ionic surfactants forms spherical cages containing from one to several hundreds of micelles in a closely packed state, as determined by Berret et al.<sup>32</sup> according to SANS, cryo-TEM, and Monte Carlo simulations. In addition, the presence of a polyelectrolyte may induce formation of cylindrical micelles of oppositely charged surfactant, as reported by Bergström et al.<sup>33</sup> due to SANS (for anionic surfactant, and polycation, SDS–poly{3-(2-methylpropionamido)propyl}trimethylammonium chloride). Thus, the polyelectrolyte may indeed act as a salt, decreasing the charge density on micelle surfaces and yielding cylindrical micelles, which are bound to the polymer chains, probably due to a combination of hydrophobic and electrostatic forces.<sup>34</sup> The arrangement of the hexagonal liquid crystal aggregates as polygonal particles with a hexagonal outer shape (Figure 4a–c, Figure 5b,c), as well as curved structures (Figure 4e, arrow in Figure 5b), indicates the formation of hexosomes. Similar observations were reported for the nonionic system composed of monolinolein, Pluronic F127, and tetradecane.<sup>35</sup> These two morphologies of the same hexagonal liquid crystal structure were explained by Sagalowicz et al.<sup>36</sup> for several systems. The particles having the hexagonal outer shape evolve from cylindrical micelles in which the longitudinal axis of the tubes forming the hexagonal liquid crystal particle remains straight. In coexistence with the hexagonal particles the tubes can become circular and ideally can be closed by each other in such a way that no tube endings are present any more. The hexagonal structure of the particles is also anticipated by preliminary computational simulation results.<sup>37</sup>

**Effect of Surfactant Chain Length.** A series of samples were prepared, in which surfactants of increasing chain lengths (constant concentration, 5 mM), were mixed at the same charge molar ratio ( $R = 0.47$ ), with polymer solutions at constant concentration (0.1% w/w, 10 mM of monomeric units). The average sizes by number distribution, as evaluated by dynamic light scattering are summarized in Table 1. It should be noted that the polymer and surfactant concentrations in this section are higher than those in the previous sections, since for some compositions (especially for short chain surfactants, at constant

**Figure 6.** Cryo-TEM images of the C<sub>n</sub>TAB–NaPA system at 0.1% polymer, 5 mM C<sub>n</sub>TAB, and charge ratio  $R = 0.47$ : (a)  $n = 10$ ; (b)  $n = 12$ ; (c)  $n = 14$ ; (d)  $n = 16$ ; inset in 'd' shows a hexagonal nanoparticle of the same system. Scale bars = 50 nm.

$R$  ratio) the quality of the cryo-TEM micrographs was not good at low concentrations.

We found that particles are formed only by chain length of 10 carbon atoms or longer, and that the average particle size increases with increased surfactant chain length. Particles were not formed by the shortest chain surfactant checked, C<sub>8</sub>TAB. That finding resembles that of Huang et al.<sup>38</sup> who found that C<sub>8</sub>TAB did not form vesicles with partially hydrolyzed polyacrylamide at all molar ratios. Thalberg et al.<sup>39</sup> evaluated the interaction between hyaluronan and cationic surfactants and noted no visual opalescence at all surfactant concentrations with surfactant hydrocarbon chains shorter than C<sub>10</sub>. Svensson et al.<sup>40</sup> reported for alkyltrimethylammonium polyacrylates salts that the attraction between polyions and surfactant aggregates also increased with increasing surfactant chain length. These findings indicate that the alkyl chain of the surfactant molecule should be sufficiently long to allow significant hydrophobic interaction with the polyelectrolyte. The formation of particles and the increase in their size with the increased chain length can be explained by more pronounced hydrophobic interactions. These results, together with our recent findings<sup>34</sup> based on binding isotherms and *ab initio* quantum mechanical calculations, for the SDS/PDAC system, support the conclusion that electrostatic attraction between polyelectrolyte and oppositely charged surfactant could not be the main driving force for binding of the surfactant to the polymer, but hydrophobic forces play an important role in this process. However, the differences in particle size while using different surfactant chain lengths could also be a result of the way the experiments were conducted, and of the changes in surfactant concentration relative to its CMC. However, an attempt to perform a similar experiment at a common concentration of surfactant, relative to its CMC (1.5 the CMC) failed, because of precipitation at all molar ratios.

The nanoparticles formed in the C<sub>10</sub>TAB–NaPA system are shown in Figure 6a. The particle size is in the order of 50 nm. In this figure we concentrated on the large particles, since we were interested in revealing the inner structure of each particle. Smaller particles could be present in the background, almost

(31) Zhang, W.; Li, G. Z.; Mu, J. H.; Shen, Q.; Zheng, L. Q.; Liang, H. J.; Wu, C. *Chin. Sci. Bull.* **2000**, *45*, 1854.

(32) Berret, J. F.; Herve, P. *J. Phys. Chem. B* **2003**, *107*, 8111.

(33) Bergström, L. M.; Kjellin, U. R. M.; Claesson, P. M. *J. Phys. Chem. B* **2004**, *108*, 1874.

(34) Nizri, G.; Lagerge, S.; Kamyshnya, A.; Major, D. T.; Magdassi, S. *J. Colloid Interface Sci.* **2008**, *320*, 74.

(35) Yaghmur, A.; De Campo, L.; Sagalowicz, L.; Leser, M. E.; Glatter, O. *Langmuir* **2005**, *21*, 569.

(36) Sagalowicz, L.; Michel, M.; Adrian, M.; Frossard, P.; Rouvet, M.; Watzke, H. J.; Yaghmur, A.; De Campo, L.; Glatter, O.; Leser, M. E. *J. Microsc.* **2006**, *221*, 110.

(37) Nizri, G.; Major, D. T.; Magdassi, S. Unpublished results.

(38) Huang, J.; Zhu, Y.; Zhu, B.; Li, R.; Fu, H. I. *J. Colloid Interface Sci.* **2001**, *236*, 201.

(39) Thalberg, K.; Lindman, B. *J. Phys. Chem.* **1989**, *93*, 1478.

(40) Svensson, A.; Normann, J.; Piculell, L. *J. Phys. Chem. B* **2006**, *110*, 10332.

indistinguishable. The average size by number using light scattering measurements (Table 1) is 4.5 nm, which reflects more accurately the population of all the particles. The inner structure of the C<sub>10</sub>TAB–NaPA particles is not as well ordered and they are not clearly faceted, compared to the C<sub>16</sub> system described above.

The system of C<sub>12</sub>TAB–NaPA, at the same concentration and charge ratio, shows much better developed hexagonal nanoparticles with apparent edges that are closer to straight lines, and with clear inner structure, as shown in Figure 6b. Particle size ranges from about 15 to 300 nm. It seems that the larger particles have better defined inner nanostructure. On the basis of measurement from calibrated FFT images of the recorded micrographs, we deduce that the characteristic distance, corresponding to the diameter of the threadlike building block of the hexagonal liquid crystal particle is about 4.5 nm.

The C<sub>14</sub>TAB–NaPA and C<sub>16</sub>TAB–NaPA systems yield nanoparticles similar to the C<sub>12</sub> system. However, the nanoparticles seem to take on more perfect hexagonal form with increasing hydrocarbon chain length of the surfactant. The building blocks of the nanoparticles seem to be somewhat larger, around 5.2 nm, but one cannot rely on the TEM data alone. In addition to small discrete nanoparticles we observe domains of thin layers of organized inner structure (arrow in Figure 6c; the larger area in Figure 6d).

It seems that the hexagonal liquid crystal inner structure of the particles becomes more pronounced with the increase in surfactant chain length. The reason for this could be related to micelle formation. As mentioned above, the dispersions of nanoparticles were prepared while using a constant polymer and surfactant concentration. Surfactant concentration was 5 mM; therefore, the concentration of surfactant relatively to the CMC was different for each surfactant. The CMC of the surfactants are 64.6, 15, 3.6, and 0.92 mM for C<sub>10</sub>TAB, C<sub>12</sub>TAB, C<sub>14</sub>TAB, and C<sub>16</sub>TAB, respectively.<sup>41</sup> It should be emphasized that those are CMC values in pure water. Accordingly, the particles of C<sub>16</sub>TAB–NaPA (Figure 6d) were prepared at surfactant concentration five times the CMC, while the C<sub>10</sub>TAB–NaPA particles (Figure 6a) were prepared at surfactant concentration only 1/13 of the CMC. Since micelles are the building blocks of the nanoparticles, it is reasonable to assume that the closer the surfactant to its CMC, the more organized is the inner structure of the particle. Moreover, as was argued above, TLMs of the surfactant are the building blocks of the hexagonal liquid crystal particles. It is generally known that there is a sphere-to-rod transition of ionic surfactant micelle shape with the increase in surfactant concentration.<sup>42</sup> This transition occurs at 0.25 M at 30 °C for C<sub>16</sub>TAB,<sup>30</sup> while it happens at much higher concentrations for surfactants with chain length shorter than 16, as reported by Mata et al.<sup>24</sup> Therefore, it seems that the more the surfactant

tends to form elongated micelles, the greater is its tendency to form perfect hexagonal liquid crystal particles in presence of the polymer.

It is interesting to compare our results with those obtained recently by Trabelsi et al.<sup>43</sup> for the interaction between carboxymethylcellulose (carboxyMC) and two surfactants, DTAB and CTAB, at several surfactant and polymer concentrations, that is, various *R* ratios. The conclusions from their work were that the inner organization of the complexes formed by the polyelectrolyte and the surfactant depends on the surfactant chain length, since a cubic organization was observed (by SANS measurements) for the carboxyMC/DTAB system, while the carboxyMC/CTAB system did not show any regular organization. However, in our system an ordered inner structure is seen in C<sub>12</sub>TAB and C<sub>16</sub>TAB systems, indicating the importance of the polymer structure to the inner organization.

## Conclusions

We investigated the formation of nanoparticles by interaction between a polycation, NaPA, and a series of cationic surfactants with various chain lengths. We found for the C<sub>16</sub>TAB–NaPA interaction that nanoparticles are formed through a wide range of surfactant concentrations. The molar charge ratio between the surfactant and polymer affects the size and zeta potential of the formed nanoparticles. The inner structure of the nanoparticles at the concentrations investigated, as revealed using cryo-TEM, was found to be of hexosomes, which are hexagonal liquid crystal particles of closely packed TLMs of C<sub>16</sub>TAB, longitudinally decorated by the polymer chains. The molar charge ratio does not have a significant effect on the inner structure of the particles. However, the chain length of the surfactant was shown to affect the particles diameter, as well as their inner structure: the larger the chain length, the larger the particles and the more ordered the hexagonal structure. It seems that the longer the surfactant hydrocarbon chain, the greater is the ability of the polymer to induce TLM formation by the surfactant, of which the hexagonal liquid crystal particles are composed. Some of these results are similar to those obtained for the oppositely charged system (a polycation and an anionic surfactant). We continue to evaluate the generality of these conclusions by a theoretical study.

**Acknowledgment.** The cryo-TEM work was performed at the Hannah and George Krumholz Laboratory for Advanced Electron Microscopy, part of the Technion Project for Complex Liquids, Microstructure and Macromolecule, with partial support from the Technion Russell Berrie Nanotechnology Institute (RBNI).

**Note Added after ASAP Publication.** This article was released ASAP on January 14, 2009. Figures 4–6 were increased in size to provide more detail, and the article was reposted on January 21, 2009.

LA8031013

(41) Mukerjee, P.; Mysels, K. J. *Critical Micelle Concentrations of Aqueous Surfactant Systems*; US Government Printing Office: Washington, DC, 1971.

(42) Tedeschi, A. M.; Franco, L.; Ruzzi, M.; Paduano, L.; Corvaja, C.; D'errico, G. *Phys. Chem. Chem. Phys.* **2003**, *5*, 4204.

(43) Trabelsi, S.; Guillot, S.; Rittaco, H.; Boue, F.; Langevin, D. *Eur. Phys. J. E* **2007**, *23*, 305.